Development of Meshing Variation Analysis of Worm Gear Used in Electric Power Steering

A. KIKUCHI S. MACHIDA

It was difficult to theoretically analyze meshing variation of the worm gear used in electric power steering by numerical formula, because gear meshing positions are largely displaced due to the structure and material. Due to this, we repeated vehicle and bench experiments and conducted countermeasures through trial and error. In order to provide a more efficient and accurate analysis, which was a challenge during product development, we worked to create a meshing variation design tool using a finite element method to allow prior estimation of gear meshing variation. As a result, we have succeeded in creating an analysis technology with correlation to actual results, which makes prior estimation in the design stage possible. In addition, we have succeeded in visualizing the shared load on each tooth surface and contact position. This has facilitated the study on reduction of meshing variation and made development more efficient.

***Key Words**: electric power steering, worm gear, gear vibration, finite element method*

1. Introduction

The rise in environmental awareness of recent years has driven the market in vehicles with high quietness, such as hybrid vehicles (HVs) and electric vehicles (EVs), and created a demand for further quietness of electric power steering (EPS). The majority of EPS adopt worm gears and an important issue is how to prevent the vibration and noise created due to meshing variation when the steering wheel is steered.

Furthermore, there is also a need for the gear to prevent the rattling noise which occurs when driving vehicles on rough roads. As such, resin is used as the material of the worm wheel and backlash is kept at zero constantly by pressing the worm against the worm wheel with a backlash adjustment mechanism. Therefore, when the assist torque from the motor is inputted into the gear during steering wheel operation, elastic deformation occurs in the sections of the worm wheel made of resin and worm displacement is caused due to the backlash adjustment mechanism, thus making it difficult to analyze the gear tooth face's state of contact. Hence, we were faced with the challenge during product development of how to achieve a more efficient and accurate analysis, and in reality, were forced to repeat vehicle and bench experiments and establish countermeasures through a process of trial and error.

Meanwhile, the finite element method (FEM), a representative technique of CAE, is able to support analysis conditions including contact of a complex shape and as such has been used as a method to evaluate the stress and contact face pressure of the meshing portion when investigating the strength and reliability of gears.

This report introduces initiatives towards building a design investigation tool which applies FEM, is able to predict meshing variation at the design stage and efficiently investigate a reduction technique. We will also introduce an example of actually using this analysis technique to investigate reduction of meshing variation.

2. The role and overview of gears

Figure 1 shows the structure of a steering system. Assist torque responding to the steering torque by the driver is generated in the motor, amplified by passing through the gear and transferred to the output axis.

Figure 2 shows the structure of a gear with a backlash adjustment mechanism.

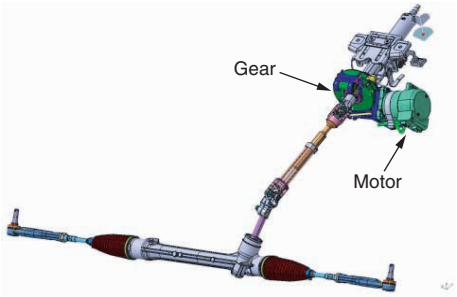

Fig. 1 Structure of steering system

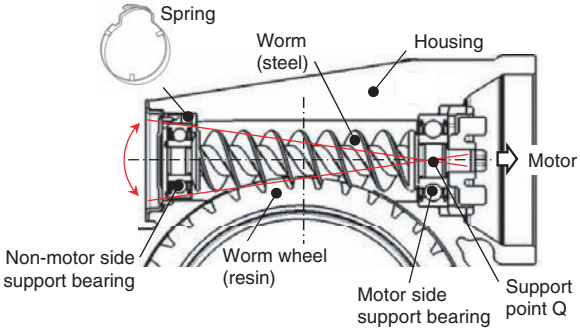

Fig. 2 Worm gear with backlash adjustment mechanism

The worm is able to become displaced centered on the support point Q, which is the center of the motor side support bearing, due to clearance secured between the worm's non-motor side support bearing and housing, and a special spring embedded for backlash adjustment. During motor operation, the inner diameter of the housing on the non-motor side acts as a stopper and restricts worm displacement.

3. Analysis technique

3. 1 Flow of analysis

It is a known fact that much of the vibration and noise generated when the steering wheel is steered has correlation with the variation in output torque of the gear. Here, we investigated calculating the variation in the output torque generated by meshing variation in the case that a constant motor assist torque was inputted. **Figure 3** provides an outline of the analysis procedure.

The worm and worm wheel models were made by preparing a processing tool model, creating a tool trajectory envelope that is generated in actual processing and removing that from the pre-processing profile model. Consequently, it is possible to prepare models from an arbitrary tool profile. Regarding the worm wheel model, we focused on the low-rigidity resin portions and created an angle scope where the worm wheel meshes with the worm with consideration to elastic deformation.

3. 2 Load and boundary conditions

After placing the worm and worm wheel models at the predetermined center distance, we meshed them at an arbitrary angle, fixed the inner diameter face of the worm wheel resin and performed static analysis while applying constant torque on the worm. For the analysis model, we combined the worm support bearing and housing in addition to the worm and worm wheel. **Figure 4** shows the applied load and boundary conditions defined in each element model.

Torque equivalent to motor torque was inputted in the worm and the worm was subjected to a reaction force due to the contact boundary with the worm wheel tooth face and the contact boundary between the non-motor side bearing and housing. Moreover, the motor side bearing and worm press-fit face is bound by a spring coupling which considers the axial rigidity, radial rigidity and angle rigidity of the bearing, and expresses the bearing support rigidity. The spring load has not been considered as it is sufficiently small compared with the housing stopper contact load at the presumed input torque.

After executing the calculation, we confirmed the rotation moment component of the output axis periphery from the reaction force generated on the worm wheel fixed face. This is equivalent to the output torque.

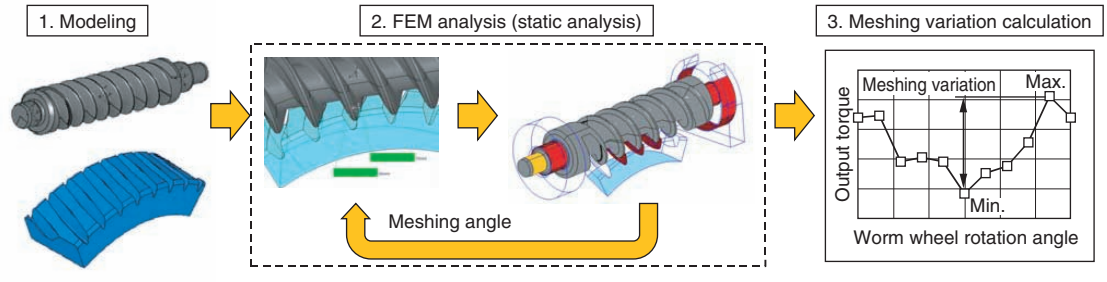

Fig. 3 Outline of analysis procedure

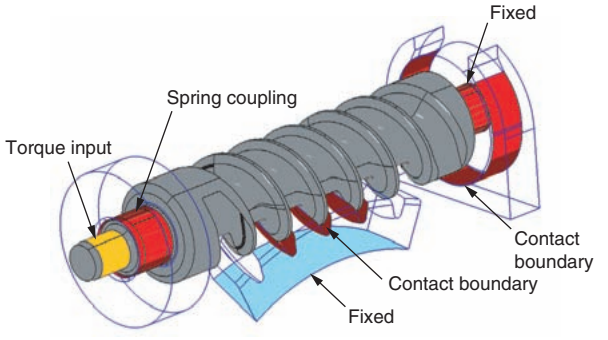

Fig. 4 Applied load and boundary conditions

3. 3 Calculating meshing variation

The abovementioned analysis was repeated while changing the meshing angle of the worm and worm wheel. For the meshing angle, the angle pitch was equally divided, and the change in output torque within one pitch rotation was discretely calculated. The difference between the maximum and minimum values of the calculated output torque was made the meshing variation.

4. Experiment verification results

In order to confirm the validity of this analysis technique, a comparison was made with the results of an actual test using a column for C-EPS®. **Figure 5** shows an outline of the examination procedure.

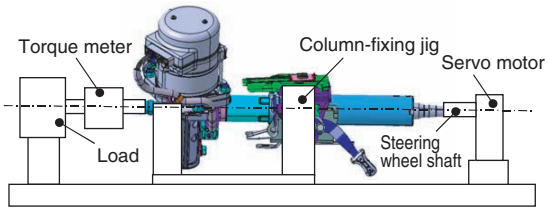

Fig. 5 Outline of examination procedure

The steering wheel shaft was turned at a constant rotation speed using the servo motor, the time axis waveform for column output torque when load was applied to the output axis was measured and the torque variation was calculated.

Figure 6 shows the measured time axis waveform of the output torque. We confirmed that the primary meshing cycle calculated from the steering wheel rotation speed and worm gear reduction ratio was consistent with the cycle of the measured output torque variation.

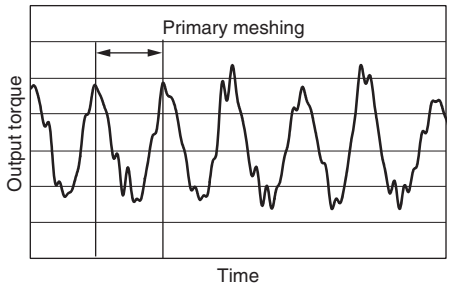

Fig. 6 Experimental data of output torque

Next, we measured the output torque variation on column assemblies with differing gear tooth specifications. At the same time, we prepared a tooth profile model of the same specifications and analyzed the meshing variation using FEM. **Figure 7** is a comparison of the measurement results and the calculation results. The correlation coefficient R^2 exceeds 0.7, and it can be deemed there is no problem in making the meshing variation calculated using the analysis technique in the previous chapter a performance index.

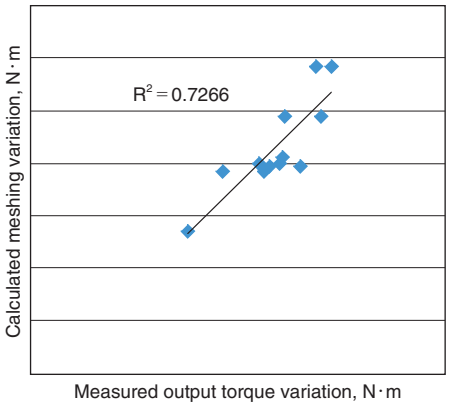

Fig. 7 Comparison of measurement results and calculation results

5. Investigation of a technique to reduce meshing variation

5. 1 Visualization of meshing variation

An important point of investigating the design specifications enabling the reduction of meshing variation is ascertaining the relationship between variation in load sharing of the contact teeth, variation in the meshing contact point, and variation in the number of teeth meshing, as well as the variation in output torque that corresponds with these. Therefore, at the same time as using the analysis technique shown in the previous chapter to calculate the meshing variation of the worm wheel axis, we used FEM analysis to find the shared load in the direction of worm wheel rotation (F_i) that occurs in the corresponding meshing of the worm and worm wheel tooth (tooth pair), as well as the contact radius (r_i). **Figure 8** provides an overview of that.

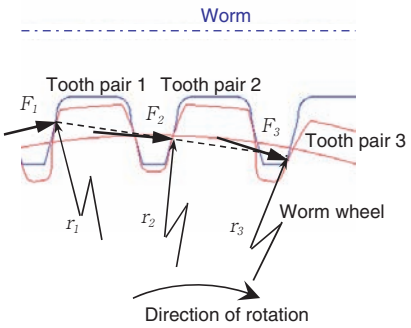

Fig. 8 Shared load and contact radius of meshing tooth

From the torque balance, output torque T would be as follows if the m tooth pair was meshing at the same time.

$$T = F_1 r_1 + F_2 r_2 + \cdots + F_m r_m \quad (1)$$

Regarding the tooth contact portion, we had made the contact radius the position where the maximum face pressure was generated due to the fact that a constant area is maintained as a result of worm wheel resin elastic deformation. We deemed there was no problem with this technique as the output torque calculated from Formula 1 and the output torque from the analysis results were in close agreement. **Figure 9** shows the transition in the shared load and contact radius of each tooth pair, as well as the output torque, when the meshing angle is changed for a gear of certain specifications.

There are changes in shared load and contact radius for the respective corresponding teeth, therefore the figure differentiates between tooth pairs 1, 2 and 3. In other words, for these particular gear specifications, a state of meshing with two teeth alternates with a state of meshing with three teeth, and the actual meshing ratio is between two and three. From **Fig. 9** (b), the shared load of "tooth pair 1" decreases as meshing progresses from the angle pitch of 0, and the output torque of **Fig. 9** (a) decreases. After this, meshing of "tooth pair 3" begins from the angle pitch of 0.6 and it can be observed that the output torque increases as the shared load increases.

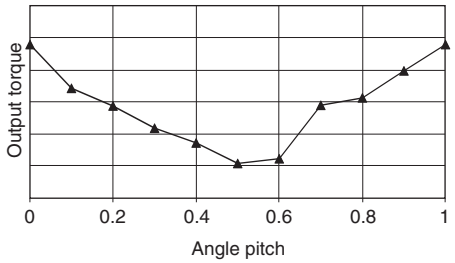

(a) Relationship between output torque and angle pitch

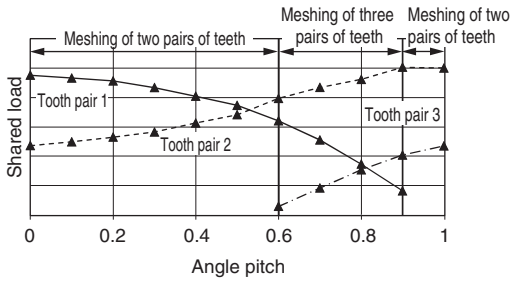

(b) Relationship between shared load of each tooth pair and angle pitch

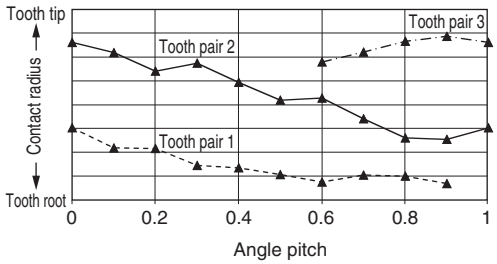

(c) Relationship between contact radius of each tooth pair and angle pitch

Fig. 9 Calculation results

5. 2 Example of a technique for reducing meshing variation

Here, as an example of a countermeasure for meshing variation, we investigated optimizing the setting angle of the hob, which is used to machine the worm wheel. If the hob setting angle when machining teeth is made β, the worm wheel lead angle is made γ and the hob lead angle is made α, the principle will be $\beta = \gamma - \alpha$ as shown in **Fig. 10**.

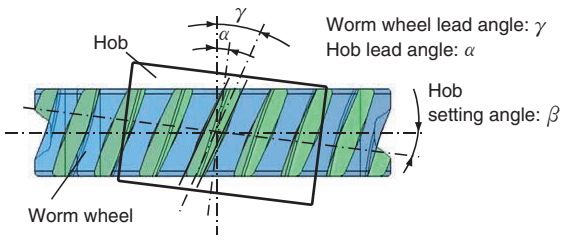

Fig. 10 Relationship between worm wheel and hob

In the case of the gear specifications in **Fig. 9**, it can be seen from **Fig. 9** (b) that the reason for the decrease in output torque is a decrease in the shared load of "tooth pair 1". "Tooth pair 1" meshes with the worm wheel tooth root therefore if the shared load at the tooth root can be maintained, the decrease in output torque can be minimized, thus reducing output torque variation. Meanwhile, the contact point with the worm in the worm wheel, as shown in **Fig. 11**, does not only progress in the radial direction but also the tooth flank direction therefore by increasing the hob setting angle β it would be possible to increase contact with the worm in the worm wheel tooth root area and it can be predicted that this would maintain shared load.

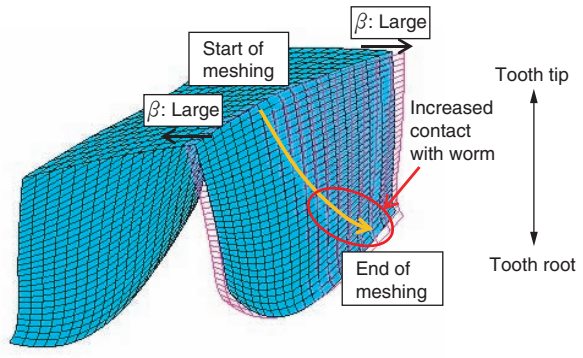

Fig. 11 Tooth surface of worm wheel and meshing line with worm

In light of this, we conducted further analysis using gear specifications with two different hob setting angles. The results of this are shown in **Fig. 12**. The relationship between the hob setting angles of β_0, β_1, and β_2 in the figure is $\beta_0 < \beta_1 < \beta_2$.

Looking at the calculation results of output torque variation, β_1 from **Fig. 12** (a) is the lowest and the cause of this is considered from the relationship between shared load and contact radius. Looking at the analysis results of β_1 from **Fig. 12** (b), it can be seen that the shared load of tooth pair 1", in comparison with β_0, has increased in the 0 to 0.6 pitch range as expected, and reduction of output torque has been minimized. However, if the hob setting angle is made as large as β_2, the output torque variation from **Fig. 12** (a) instead becomes larger than β_0. When shared load and contact radius are compared with other specifications, the reduction in output torque for β_2 is minimized for the first half of the angle pitch however the angle at which meshing of "tooth pair 3" starts is later than other specifications and this is due to a delay of a rise in output torque. This is because, if the hob setting angle increases, on the worm wheel tooth tip side, in other words at the beginning of meshing, the tooth profile changes in the direction whereby the clearance with the worm increases. This is expressed in **Fig. 11**.

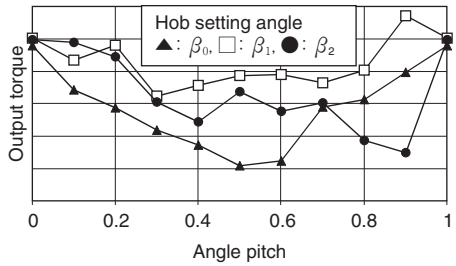

(a) Relationship between output torque and angle pitch

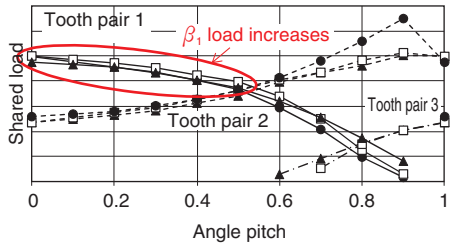

(b) Relationship between shared load of each tooth pair and angle pitch

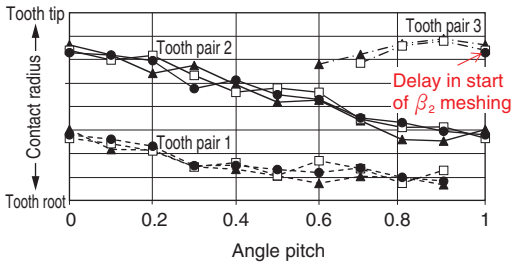

(c) Relationship between contact radius of each tooth pair and angle pitch

Fig. 12 Hob setting angle and meshing variation

In this way, it is possible to find the optimal hob setting angle in relation to meshing variation and even in an actual verification, as shown in **Fig. 13**, a 30% reduction in output torque variation compared with conventional specifications was observed.

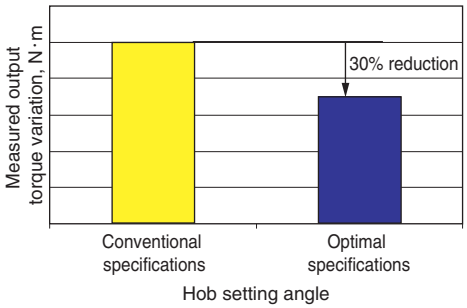

Fig. 13 Effects of optimization of hob setting angle

6. Conclusion

This paper has introduced technology for analyzing worm gear meshing variation using FEM and an examination case for reducing such variation. As explained at the outset, the meshing of worm gears for EPS is a complex phenomenon and experimental verification was difficult. However, by using the analysis technology introduced in this paper, it was possible to visualize meshing variation and easily understand and explain the phenomenon. Moreover, because it is now possible to predict meshing variation, the efficiency of development tasks can be increased by reducing man-hours in the prototype and evaluation phases. JTEKT wishes to continue development so that we may promptly respond to high-level requirements from our customers by utilizing a variety of analysis technologies.

References

1) T. Sugiura: Backlash Adjustment Mechanism for Reduction Gear of Electric Power Steering System, JTEKT ENGINEERING JOURNAL, No. 1001 (2006) 73.
2) S. Nishimura: Development of Rattle Noise Analysis Technology for Column Type Electric Power Steering Systems, JTEKT ENGINEERING JOURNAL, No. 1009 (2001) 66.

A. KIKUCHI* S. MACHIDA**

* *Component Development Dept., Steering Systems Operations Headquarters*
** *Experiment & Analysis Dept. 1, Steering Systems Operations Headquarters*